Article | Received 21 May 2025; Revised 13 October 2025; Accepted 15 October 2025; Published 24 October 2025
https://doi.org/10.55092/am20250009

Design of honeycomb energy-absorbing box and its low-speed crashing behaviour for automobiles

Wenqiang Yue, Xinlin Wang*, Xiaochi Wang and Tianmin Guan

School of Mechanical Engineering, Dalian Jiaotong University, Liaoning, China

* Correspondence author; E-mail: wxl_me@djtu.edu.cn.

Highlights:

- Novel PEEK honeycomb filler enhances crashworthiness and lightweight design.
- Regular hexagonal PEEK filler increases mean crash load by 18.1%.
- Square cross-section exhibits optimal energy absorption and load stability.
- ANSYS LS-DYNA simulation validates structural efficiency and deformation modes.

Abstract: This study investigates the application potential of high-performance lightweight materials in automotive energy-absorbing structures. The crash performance of energy-absorbing boxes with different materials and cross-sectional shapes was first evaluated using the LS-DYNA module in ANSYS Workbench, based on key energy absorption criteria. Subsequently, the low-speed crash characteristics of boxes filled with re-entrant and regular hexagonal polyetheretherketone (PEEK) honeycombs were systematically compared with a baseline hollow design and a conventional aluminum foam-filled structure. The results demonstrate that the regular hexagonal PEEK honeycomb-filled structure exhibits superior overall crashworthiness. It achieved an average crash load of 68.04 kN, which is 18.1% higher than that of the hollow design, while maintaining a lower peak load and enhanced structural stability throughout the crushing process. In contrast, although the aluminum foam filler provided high total energy absorption, it incurred a significant peak load and weight penalty. The findings indicate that the PEEK honeycomb filler offers an excellent balance between lightweight design and crashworthiness, providing a theoretical basis for its engineering application in automotive crash protection systems.

Keywords: PEEK; energy-absorbing box; honeycomb structure; low-speed crash

1. Introduction

When a vehicle collision occurs, the front-end components (e.g., bumper beam, energy-absorbing box, and front side rails) absorb impact energy through controlled plastic deformation. This mechanism reduces energy transfer to the passenger compartment, enhancing occupant protection [1]. Statistical data indicate that vehicle collisions account for over 69.9% of traffic accidents, with the majority occurring at low speeds [2]. Therefore, optimizing the design of energy-absorbing boxes to achieve high energy absorption efficiency, low initial peak load, and a stable crushing process during low-speed collisions is crucial for enhancing passive safety. However, most current energy-absorbing boxes utilize simple square or circular tubular structures, which exhibit limitations including high initial peak loads and significant load fluctuations during crushing.

To overcome the limitations of traditional energy-absorbing boxes, incorporating internal fillers represents an effective strategy. Honeycomb structures serve as ideal filler matrices due to their excellent specific stiffness/strength, controllable deformation modes, and efficient energy dissipation capacity [3]. Similarly, porous fillers (e.g., foams) have been shown to significantly enhance energy absorption. Extensive research demonstrates that honeycomb or porous fillers markedly improve the energy absorption performance of such structures. For example, polyurethane foam, carbon fiber-reinforced composites, and CF/PA6 composite filaments effectively enhance structural stability, reduce peak loads, increase specific energy absorption (SEA), and generate synergistic effects exceeding the sum of individual component properties [4–6]. Aluminum foam fillers can substantially enhance energy absorption (up to 100% [7]), reduce peak crash forces [8–10], and alter thin-walled structure deformation modes [11]. Recently, Zhao *et al.* [12] demonstrated that composite material blocks (CMB) comprising carbon fiber reinforced plastic (CFRP) negative Poisson's ratio (NPR) honeycombs filled with aluminum foam exhibit SEA values significantly surpassing the sum of individual components. This indicates a strong synergistic effect ($1 + 1 > 2$) and elucidated critical skeleton-filler coupling mechanisms. Functionally graded designs (e.g., graded honeycombs [13], graded aluminum foam [14]) and sandwich structures (e.g., aluminum foam/aramid epoxy [15]) further optimize energy absorption under specific loading conditions (e.g., blast, impact). Reid *et al.* [16] established that filler enhancement effects surpass those of traditional structures. Additive manufacturing (e.g., 3D printing) enables new applications of complex honeycombs like Kagome structures [17] and continuous fiber-reinforced thermoplastic composite (CFRTPC) honeycombs [18] in energy-absorbing systems. These studies collectively indicate that novel manufacturing processes with specific materials achieve excellent ductile deformation, suppress crack propagation, and significantly enhance compressive strength and energy absorption. For instance, additively manufactured CFRTPC honeycombs yield an 86.3% increase in compressive strength and 100% improvement in energy absorption with minimal continuous fiber addition [18]. Research also focuses on structural improvements like multi-cell designs [19], optimized lantern-type configurations [20], and surrogate-based lightweight approaches [21] to enhance inherent energy absorption efficiency. The finite element method (FEM), with its accurate mechanical models, efficient algorithms, and high-fidelity crash simulation capabilities, has become a core design/optimization tool [22]. Owing to significant advantages in shortening R&D cycles, reducing costs, and minimizing physical testing, FEM is widely applied to predict energy-absorbing box performance [23], optimize parameters (e.g., transition fillet radii), and validate filler structure effectiveness [24].

However, existing filling strategies face limitations in balancing lightweight design and crashworthiness. Metallic foams have high density, while some lightweight polymers may compromise strength or thermal stability. To bridge this gap, this study pioneers the application of polyether ether ketone (PEEK) as the honeycomb core material. PEEK is an advanced thermoplastic known for its exceptional specific strength, toughness, impact resistance, thermal stability, and low density (approximately one-third of aluminum alloys) [25]. This strategy addresses the limitations of both metallic foams and conventional polymers. Furthermore, while previous studies focused on metallic honeycombs or polymer foams, the coupling mechanism between PEEK and different topological configurations (e.g., regular hexagonal *vs.* re-entrant) and its impact on crashworthiness remain largely unexplored.

Therefore, this work systematically investigates the low-speed impact performance of PEEK honeycomb-filled boxes. Using the ANSYS Workbench/LS-DYNA platform, we compare the performance of PEEK honeycomb-filled boxes (with re-entrant and regular hexagonal topologies) against conventional hollow designs, focusing on energy absorption, specific energy absorption (SEA), peak load, and mean load. This research aims to clarify the advantages of PEEK honeycomb structures and provide theoretical support for their application in automotive safety.

2. Parameters for evaluating the crashworthiness of energy-absorbing boxes

2.1. Energy absorption evaluation metrics

In the event of a vehicle collision, the primary metrics for evaluating the crashworthiness of energy-absorbing boxes include:

(1) Total energy absorption EA_T

Total energy absorption EA_T refers to the sum of energy absorbed by the energy-absorbing box through elasto-plastic deformation during the entire impact event, expressed as the integral of the crush force with respect to the compressive displacement.

$$EA_T = \int F_S \mathrm{d}s \ \ (1) \tag{1}$$

F_S—Instantaneous impact force corresponding to displacement s (N).

(2) Specific energy absorption *SEA*

Specific energy absorption *SEA* denotes the impact energy absorbed per unit mass of the energy-absorbing box. It is defined as the ratio of the total energy absorption to the total mass of the box.

$$SEA = \frac{EA_T}{M} \tag{2}$$

SEA is an indicator that combines structural safety and strength. A larger *SEA* indicates a higher efficiency of material utilisation.

(3) Average load F_{av}

Average Load F_{av} represents the mean value of the load acting on the energy-absorbing box during the impact. It is defined as the energy absorbed per unit displacement of the box, expressed as the ratio of the total energy absorption EA_T to the compressive displacement S:

$$F_{\mathrm{av}} = \frac{EA_T}{S} \tag{3}$$

Compressive Displacement is the longitudinal compression generated by the energy-absorbing box during the collision. Its value reflects the energy absorption efficiency. While greater compression can enhance energy absorption, the physical limits of the box must be considered: excessive compression cannot fully guarantee sufficient survival space for the occupants. Therefore, the value of s should be constrained within a reasonable range to ensure adequate survival space.

(4) Peak load F_{max}

Peak Load F_{max} refers to the maximum load recorded during the collision process.

The peak load directly determines the vehicle's deceleration during impact. To ensure passenger safety, F_{max} should be minimized.

This study analyzed the energy absorption characteristics of honeycomb-filled energy-absorbing boxes using three key metrics: specific energy absorption *SEA*, average load F_{av}, and peak crush load F_{max}.

3. Influence of material and cross-sectional shape on crashworthiness of energy-absorbing boxes

3.1. Effect of material selection on the energy absorption characteristics of automotive energy-absorbing boxes finite element model setup

3.1.1. Low-speed crash simulation of rectangular low-carbon steel boxes

Based on a rectangular thin-walled energy-absorbing box from a passenger car, a finite element model was established (Figure 1). The energy-absorbing box has dimensions of 108 mm (length) × 76 mm (width) × 157 mm (height), with a uniform wall thickness of 2 mm. Automotive structural steel SAPH440 was used as the box material [26].

The material parameters of the automotive structural steel SAPH440 selected in this paper were obtained from the literature [27] and are shown in Table 1.

Table 1. SPAH440 material properties.

Density (kg/m^3)	Elastic modulus (GPa)	Poisson's ratio	Yield stress (MPa)	Tangent modulus (MPa)
7.81×10^3	207	0.31	326	2070

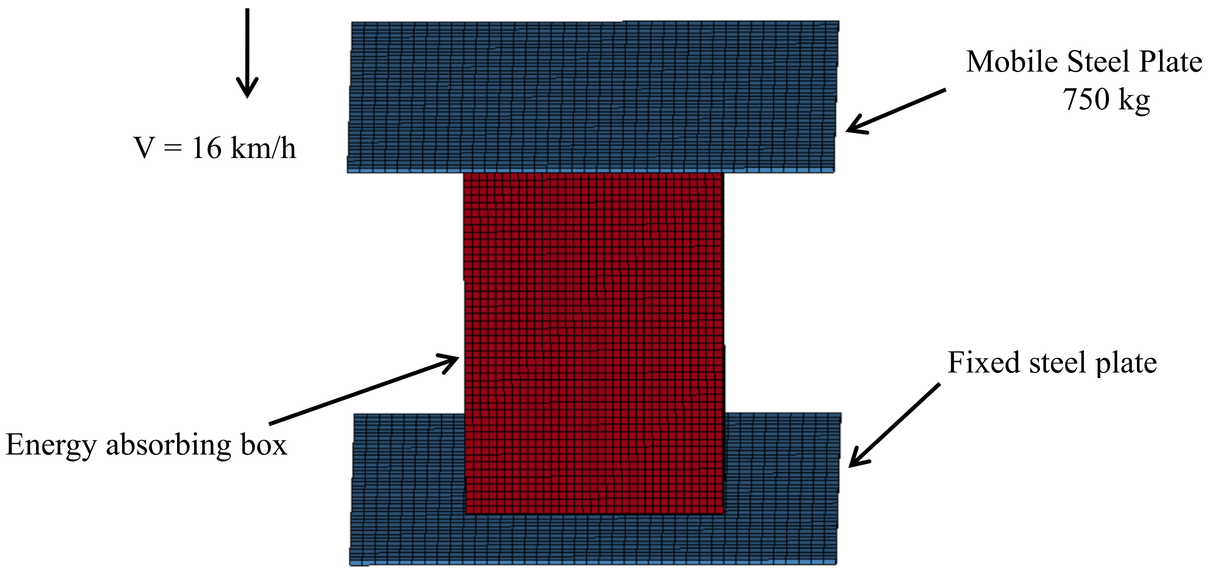

Figure 1. Rectangular energy-absorbing box low-speed crash simulation model.

In this model, two rigid planes were defined: one as the moving plate and the other as the fixed plate for the energy-absorbing box. The simulation was performed using ANSYS Workbench LS-DYNA. Resultant d3plot files were imported into LS-PrePost for post-processing. The energy-absorbing box was positioned between the fixed and moving plates. The moving plate had a mass of 750 kg and an impact velocity of 16 km/h [28], with a simulation duration of 0.06 s. Geometric contact interactions were defined between the two rigid planes and the energy absorption box, with the penalty method employed as the contact algorithm for all interfaces. The static and kinetic friction coefficients were uniformly set to 0.2 for all structures. Additionally, AUTOMATIC_SURFACE_TO_SURFACE contact was implemented between the energy absorption box and the moving steel plate. To prevent self-penetration of the energy absorption box during the crash event, the AUTOMATIC_SINGLE_SURFACE contact algorithm was applied. The energy absorption box was bound to the surface of the fixed steel plate using CONSTRAINED_EXTRA_NODES_SET. A rigid body constraint was applied to the fixed steel plate, specifically fixing all six degrees of freedom. In the simulation, the shell of the energy-absorbing box employed the Belytschko-Tsay formulation, utilizing single-point integration in the plane and five integration points through the thickness [29]. The energy-absorbing box was meshed with 3 mm quadrilateral elements, while the rigid walls used 5 mm quadrilateral elements. Geometric strain-based element erosion was activated in LS-DYNA with a maximum principal strain threshold of 0.8 [30]. Elements exceeding this critical distortion value were automatically deleted to prevent computational instability due to negative volume. It should be noted that LS-DYNA's default hourglass control coefficient (QH) is 0.1, and values exceeding 0.15 may introduce significant solution errors. Automotive crash simulations must account for inertial effects, where mass scaling influences result accuracy. The mass scaling was therefore controlled within 5% [31] to limit computational error. In this study, mass scaling parameters were set with an end time of 0.06 s, time step scale factor of 0.9, and maximum cycle count of 10^7. Through these parameter configurations, a reliable low-speed crash simulation model for the energy-absorbing box was established.

Figure 2 illustrates the progressive deformation process (images a–e) of the SAPH440 rectangular energy-absorbing box and its corresponding collision load-time curve. For clarity in depicting the deformation details, the two rigid walls are omitted from the figure. Combining the results from Figures 2 and Figure 3 revealed that: the peak load of this energy absorption box reached 246 kN, with a total energy absorption of 7140 J; at 49.8 ms into the impact, the box attained its maximum compression displacement of 102.93 mm. Observing the deformation process in Figure 2a–e shows that upon impact, the box initially develops wrinkles in its central region. As the compression displacement increases, its lower end undergoes symmetric compression, while its long sides buckle inward and its wide sides fold outward. The energy-time curve in Figure 3 further indicates that the impact kinetic energy was efficiently converted into and dissipated as internal energy, which is the mechanism enabling the total energy absorption of 7140 J. Additionally, the model's hourglass energy (97 J) and sliding interface energy (144 J) were both below 5% of the total energy [32], effectively validating the computational accuracy and result reliability of this low-velocity impact simulation model. In summary, this energy absorption box absorbed the vast majority of the impact energy through this orderly folding deformation mode, thereby achieving its purpose of protecting occupant safety and critical vehicle components.

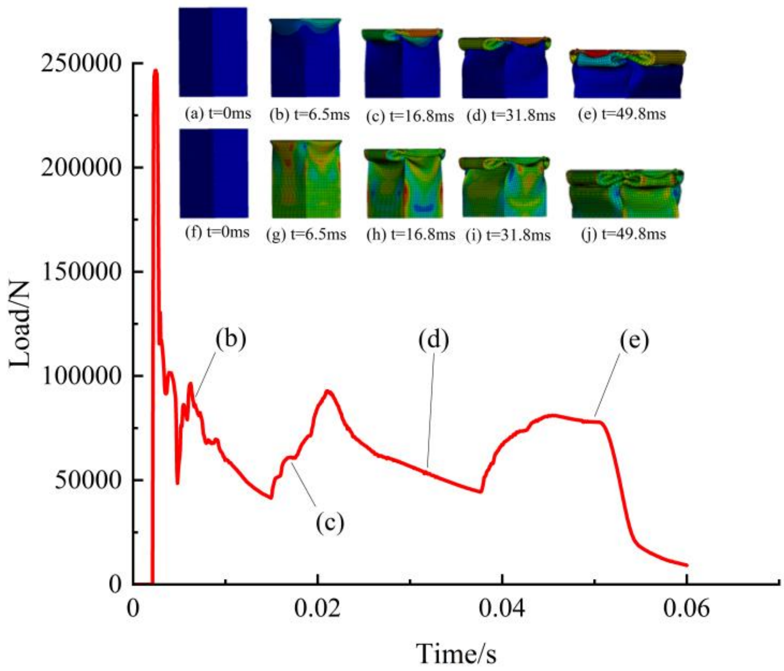

Figure 2. Low-speed crash response of rectangular SPAH440 low-carbon steel energy-absorbing box: **(a–e)** deformation modes; **(f–j)** corresponding stress maps, and crash load-time curve.

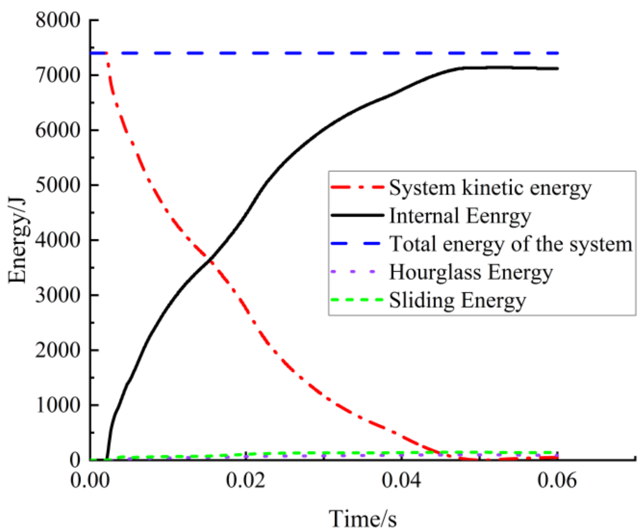

Figure 3. Energy-time curve of the rectangular SPAH440 low-carbon steel energy-absorbing box.

3.1.2. Low-speed crash simulation of rectangular aluminum alloy energy-absorbing boxes

From the SPAH440 rectangular energy-absorbing box crash load-time curve, the peak load of the box reached 246 kN. Excessive peak loads may result in damage to critical vehicle components. Therefore, it is important to ensure that the peak load of the energy absorbing box is within a certain range. In this paper, the peak load will be reduced by replacing the energy absorbing box material. Compared with low-carbon steel, aluminum alloy is characterized by its lightweight and high-strength properties. When 6061 aluminum alloy undergoes solution heat treatment followed by artificial aging (T6 temper), it exhibits excellent comprehensive mechanical properties, combining good wear resistance and processability. These attributes make it widely applicable in aerospace and automotive industries. The material parameters of 6061-T6 aluminum alloy in this paper are obtained from the paper [33] and are shown in Table 2 below.

Figure 4 illustrates the dynamic deformation process and the corresponding load-time curve of a rectangular energy-absorbing box made of AA6061-T6 aluminum alloy under low-speed crash. Figure 5 presents its energy-time curve. As shown in Figure 4a–e, outward-extending wrinkles initially form at the contact area with the rigid wall. Subsequently, a symmetrical deformation pattern develops, ultimately reaching the densification stage. The load curve exhibits a second peak; this occurs because the increased compression displacement of the aluminum alloy energy-absorbing box due to the material change leads to densification.

Table 2. 6061-T6 material properties.

Density (kg/m^3)	Elastic modulus (GPa)	Poisson's ratio	Yield stress (MPa)	Tangent modulus (MPa)
2.75×10^3	70	0.3	251	700

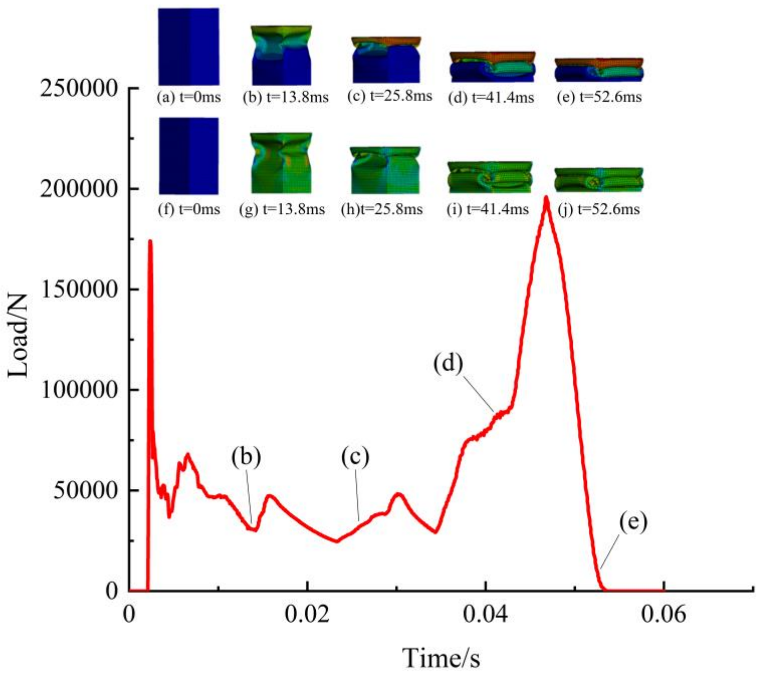

Figure 4. Low-speed crash response of rectangular 6061-T6 aluminum alloy energy-absorbing box: **(a–e)** deformation modes; **(f–j)** corresponding stress maps, and crash load-time curve.

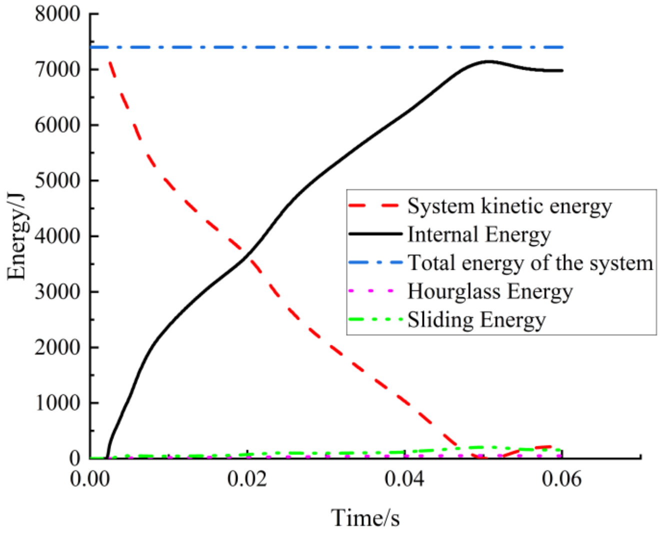

Figure 5. Energy-time curve of the rectangular 6061-T6 aluminum alloy energy-absorbing box.

3.1.3. Comparative analysis of material selection and determination

A comparative analysis of the crash performance of the rectangular energy-absorbing boxes made from SPAH440 steel and 6061-T6 aluminum alloy was conducted based on the key energy absorption evaluation parameters listed in Table 3.

Table 3. Comparative analysis of crashworthiness between rectangular 6061-T6 aluminum alloy and SPAH440 low-carbon steel energy-absorbing boxes.

Makings	Mass (g)	Total energy absorption (J)	Specific energy absorption (J/g)	Compression displacement (mm)	Peak load (kN)	Average load (J/mm)
SPAH440	882.84	7140	8.09	102.93	246	69.37
6061-T6	310.86	7160	23.03	131.99	196	54.25

The analysis reveals that although the aluminum alloy energy-absorbing box exhibits total energy absorption comparable to that of the steel counterpart (7160 J *vs.* 7140 J), it demonstrates significant advantages in other critical aspects. The aluminum alloy design achieves a remarkable mass reduction of approximately 64.7% (310.86 g *vs.* 882.84 g). More importantly, it exhibits a superior specific energy absorption (SEA) of 23.03 J/g, which is about 2.85 times higher than that of the steel structure, indicating much more efficient material utilization. Furthermore, the peak load is significantly reduced from 246 kN to 196 kN, a decrease of about 20.3%, which is beneficial for protecting key vehicle components during a collision.

In summary, 6061-T6 aluminum alloy is selected as the shell material for the energy-absorbing box in this study due to its good energy absorption capacity, significant lightweight advantage, and gentler force transmission characteristics. However, the secondary peak load observed in the rectangular section during the later collision stage (Figure 4) indicates that its load stability still has room for improvement. Therefore, the influence of different cross-sectional shapes on energy absorption performance will be investigated next.

3.2. Influence of cross-sectional shape on energy absorption characteristics

Following the material selection, the low-speed crash performance of thin-walled energy-absorbing boxes with different cross-sectional shapes—square, circular, and regular hexagonal—was compared under an equal-perimeter constraint. The key dimensions for each section are provided in Table 4.

Table 4. Dimensions (side length/diameter) of energy-absorbing boxes with identical wall thickness and different cross-sectional shapes.

Geometry	Square	Orbicular	Regular hexagon
Sizes (mm)	92	117.19	61.3

Figure 6 illustrates the deformation patterns of the energy-absorbing boxes with different cross-sections at various time instants during the crash event. The corresponding crash load-time curves are presented in Figure 7, and a comparison of key performance parameters is summarized in Table 5.

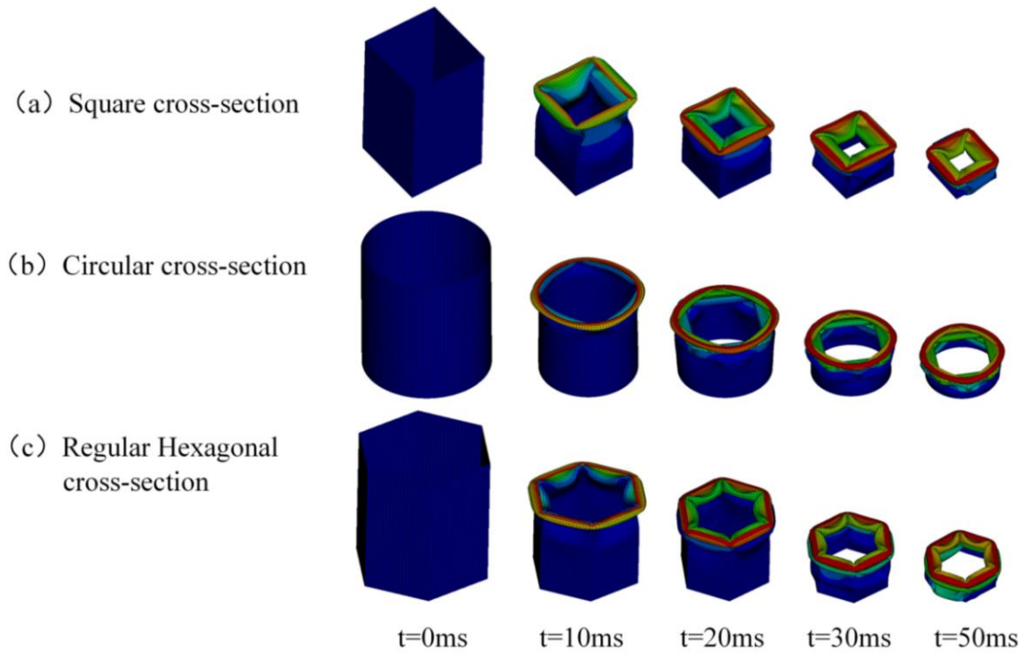

Figure 6. Deformation patterns of automotive energy-absorbing boxes with different cross-sectional shapes at various time instants. **(a)** square cross-section; **(b)** circular cross-section; **(c)** regular hexagonal cross-section.

The analysis of the deformation patterns, load curves, and performance parameters leads to the following insights. The circular section exhibits a typical axisymmetric ring-type crushing pattern. While the process is stable, it results in the highest initial peak load (190 kN) among the compared sections and shows a secondary peak in the load curve. The crushing pattern of the regular hexagonal section is intermediate between the circular and square sections, but its performance metrics, including a peak load of 178 kN and a specific energy absorption of 22.87 J/g, are slightly inferior to those of the square section.

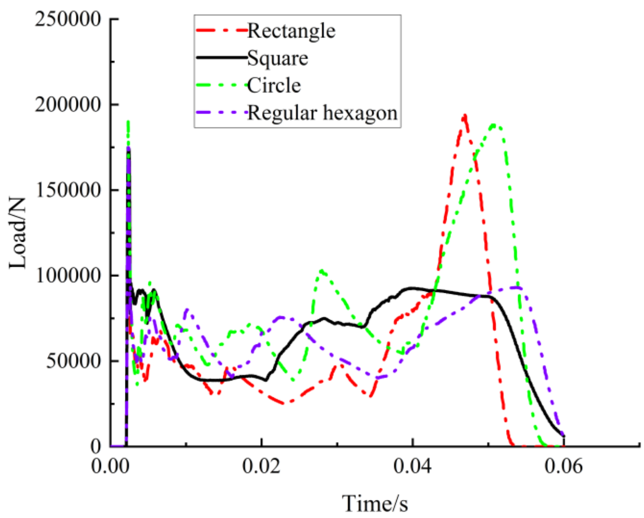

Figure 7. Crash load-time curves of automotive energy-absorbing boxes with different cross-sectional shapes.

Table 5. Comparison of crash performance parameters for thin-walled automotive energy-absorbing boxes with different cross-sectional shapes.

Section shape	Peak load (kN)	Compression displacement (mm)	Total energy absorption (J)	Specific energy absorption (J/g)	Average load (kN)
Rectangles	196	131.99	7160	23.03	54.25
Square	174	124.65	7180	23.09	57.60
Orbicular	190	122.14	7090	22.80	58.04
Regular hexagon	178	129.94	7110	22.87	54.71

In contrast, the square cross-section demonstrated the most comprehensive crash performance. Its classical diamond-shaped folding pattern (Figure 6a) ensures stable and progressive crushing. Crucially, it achieves the lowest peak load (174 kN) and the highest values for both total energy absorption (7180 J) and specific energy absorption (23.09 J/g). Furthermore, its load-time curve after the initial peak is more stable compared to the other sections (Figure 7).

Comprehensive analysis indicates that the square section performs optimally in terms of peak load, total energy absorption, and specific energy absorption, while also exhibiting a stable deformation mode. It is therefore selected as the base structure for subsequent filling with honeycomb cores. To further enhance its load stability and spatial energy absorption efficiency, the next section will investigate the effect of filling it with a PEEK honeycomb structure.

4. Design and crash performance analysis of automotive honeycomb-filled energy-absorbing boxes

4.1. Honeycomb structure design and model validation

As one of the most typical auxetic structures (*i.e.*, structures with a negative Poisson's ratio), the re-entrant honeycomb exhibits superior crash resistance and exceptional energy absorption efficiency. In this section, we first investigate the re-entrant honeycomb structure, thereby deriving the geometry of the regular hexagonal honeycomb based on identical relative density. The design guidelines for honeycomb refer to ASTM C364 (Standard Test Method for Edgewise Compressive Strength of Sandwich Construction) and ASTM C365 (Standard Test Method for Flatwise Compressive Strength of Sandwich Construction). Negative Poisson's ratio honeycomb single cell dimensions: 10 mm for vertical beams, 5 mm for inclined beams, − 30° angle of inclined beam concavity, 0.67 mm wall thickness, the specific single cell dimensions are shown in Figure 8.

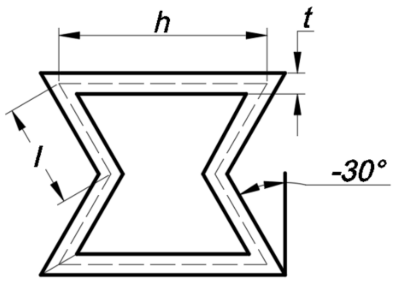

Figure 8. Schematic structure of a single-cell meta-re-entrant honeycomb.

In porous periodic structures, the relative density serves as a critical parameter for evaluating mechanical properties and facilitating cross-structural comparisons. It is defined as the volume ratio of solid material within the minimum repeating unit to the representative volume of that unit. For two-dimensional periodic structures, this ratio simplifies to the area fraction of solid material relative to the total unit area. Thus, the relative density formula for hexagonal honeycomb structures is given by [34]:

$$\rho_{\mathrm{c}} = \frac{V_{\mathrm{a}}}{V_0} = \frac{S_{\mathrm{a}}}{S_0} = \frac{(t/l)(\mathrm{h/l}+2)}{2\cos\theta(h/l+\sin\theta)} \tag{4}$$

Where ρ_c is the relative density of the negative Poisson's ratio structure; V_a, S_a are the volume and area of space occupied by all structural walls in the smallest repeating unit of the structure in units of, respectively mm^3, mm^2; V_0 , S_0 are the characterised volume, area of the smallest unit of the structure, in units, respectively mm^3, mm^2. Substituting the negative Poisson ratio cellular cell size parameters in this article into Equation (4) can get: $\rho_c = 0.2$.

Relative density constitutes a critical parameter for honeycomb structures, governing key mechanical properties such as elastic modulus, stress, and densification strain [35]. Thus, prior to comparing the energy absorption characteristics of different honeycomb configurations, the principle of controlled variables must be applied to ensure identical relative densities across all structures.

In this paper, we adopt the ortho-hexagonal honeycomb structure, *i.e.* unit cell size $l = h$. For the honeycomb structure based on the thickness of the cytosol [36], using the ortho-hexagonal unit cytosol as a reference. As shown in Figure 9 (b). Let the length of the projection of the diagonal cell arm in the horizontal direction be.

$$W = W_0 \tag{5}$$

Where, W_0 is the length of the projection of the oblique cell arm of the ortho-hexagonal unit cell element in the horizontal direction. The shape factor of this hexagonal unit cell element can be expressed as follows.

$$r_s = \frac{h}{l} = 2\sin\theta \tag{6}$$

h, l and θ are interrelated. When h is constant, the size of l can be found by varying θ, *i.e.*

$$l = \frac{w_0}{\sin\theta} = \frac{h}{2\sin\theta} \tag{7}$$

Substitute Equation (6) into Equation (7):

$$\rho_1 = \frac{2}{3}\frac{\mathrm{t}}{\mathrm{h}}\frac{\sin\theta + 1}{\cos\theta} \tag{8}$$

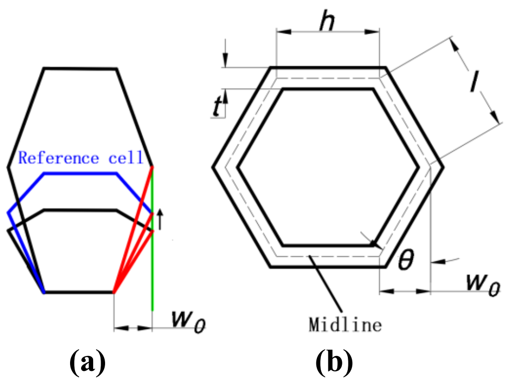

Figure 9. Geometrical characteristics of hexagonal unit cell elements. **(a)** hexagonal cell; **(b)** regular hexagonal cell (Adapted from [36]).

According to Equation (8), with reference to the parameters of the re-entrant honeycomb structure. Without changing the size of the single cell dimensions of the honeycomb such that its relative density $\rho_1 = \rho_c$, then the corresponding wall thickness of the regular hexagonal honeycomb with equal relative density is $t_1 = 0.87$ mm.

To validate the finite element model, a scaled-down specimen was tested according to GB/T 1453-2005 using a WDW-50D universal testing machine at a constant speed of 2 mm/min. As shown in Figure 10, the simulation results agree well with the experimental data in terms of both the stress-strain response and deformation pattern. This consistency underscores the fidelity of the finite element model in capturing the compressive mechanical behavior of the regular hexagonal honeycomb structure, confirming its reliability for subsequent crashworthiness analysis of the honeycomb-filled energy-absorbing boxes.

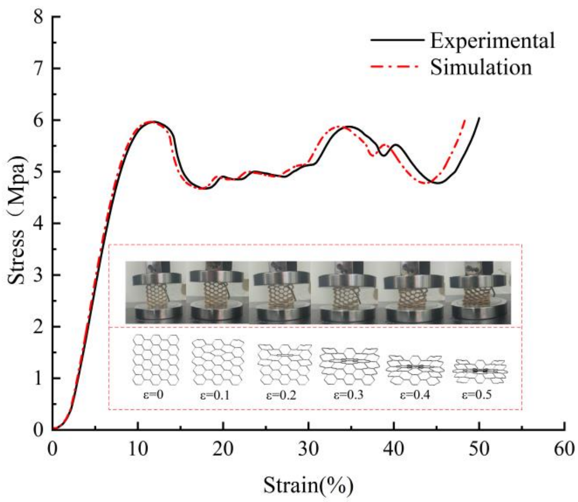

Figure 10. A comparison of finite element simulation and experimental results with deformation patterns for the regular hexagonal honeycomb structure.

4.2. Performance analysis of filled structures

A mesh sensitivity analysis was conducted on the PEEK regular hexagonal honeycomb-filled energy-absorbing box assembly (Table 6). The results indicated that a mesh size of 3 mm provided convergent results, and this size was adopted for all subsequent simulations.

Table 6. Results of the mesh sensitivity analysis for the regular hexagonal PEEK honeycomb-filled energy-absorbing box.

Mesh size (mm)	Peak load (kN)	Variation (%)	Total energy absorption (J)	Variation (%)
4	182	0	6480	0
3	176	−3.3	6700	+3.4
2	174	−1.1	6750	+0.75

The square aluminum alloy energy-absorbing box was filled with three types of cores: a re-entrant honeycomb, a regular hexagonal honeycomb, and—for broader performance benchmarking—closed-cell aluminum foam with a density of 0.54 g/cm³. The material properties of the aluminum foam are provided in Table 7. All filler cores were adhesively bonded to the inner wall of the box to ensure deformation compatibility. The honeycomb cores had the following dimensions: the re-entrant type measured 87.76 mm (X) × 87.5 mm (Y) × 156.55 mm (Z), and the regular hexagonal type measured 87.45 mm (X) × 87.5 mm (Y) × 156.75 mm (Z). The aluminum foam fully occupied the internal cavity of the box. In the finite element (FE) model, all structures were discretized using quadrilateral Belytschko-Tsay shell elements with a uniform size of 3 mm. The original energy-absorbing box contained 12,336 nodes and 8866 elements. The re-entrant and regular hexagonal honeycomb fillers comprised 60,121 nodes (37,916 elements) and 29,440 nodes (21,691 elements), respectively, while the aluminum foam was modeled with a corresponding number of solid elements. The box shell was assigned 6061-T6 aluminum alloy, and the filler materials (PEEK honeycomb and aluminum foam) were defined using the properties listed in Table 7. Strain rate effects were neglected for both filler materials under low-speed impact conditions. PEEK is noted for its low density (about one-third of aluminum alloys) and high specific strength, offering notable advantages in weight reduction and mechanical performance. Contact was defined using AUTOMATIC_SURFACE_TO_SURFACE between the impactor and the energy-absorbing box, and AUTOMATIC_SINGLE_SURFACE was applied to prevent self-penetration. The box base was fixed to the rigid plate via CONSTRAINED_EXTRA_NODES_SET. The filler cores were aligned with the bottom inner surface of the box. Static and kinetic friction coefficients were set to 0.2 for all contacts. All other loading and boundary conditions remained consistent with those of the unfilled model. The deformation patterns of the three filled configurations are illustrated in Figure 11a–c.

Table 7. Material properties of the filler cores (PEEK honeycomb and aluminum foam).

Density (kg/m^3)	Elastic modulus (GPa)	Poisson's ratio	Yield stress (MPa)	Tangent modulus (MPa)
1.28×10^3	3.6	0.38	90	180
0.54×10^3	0.7	0.33	87	100

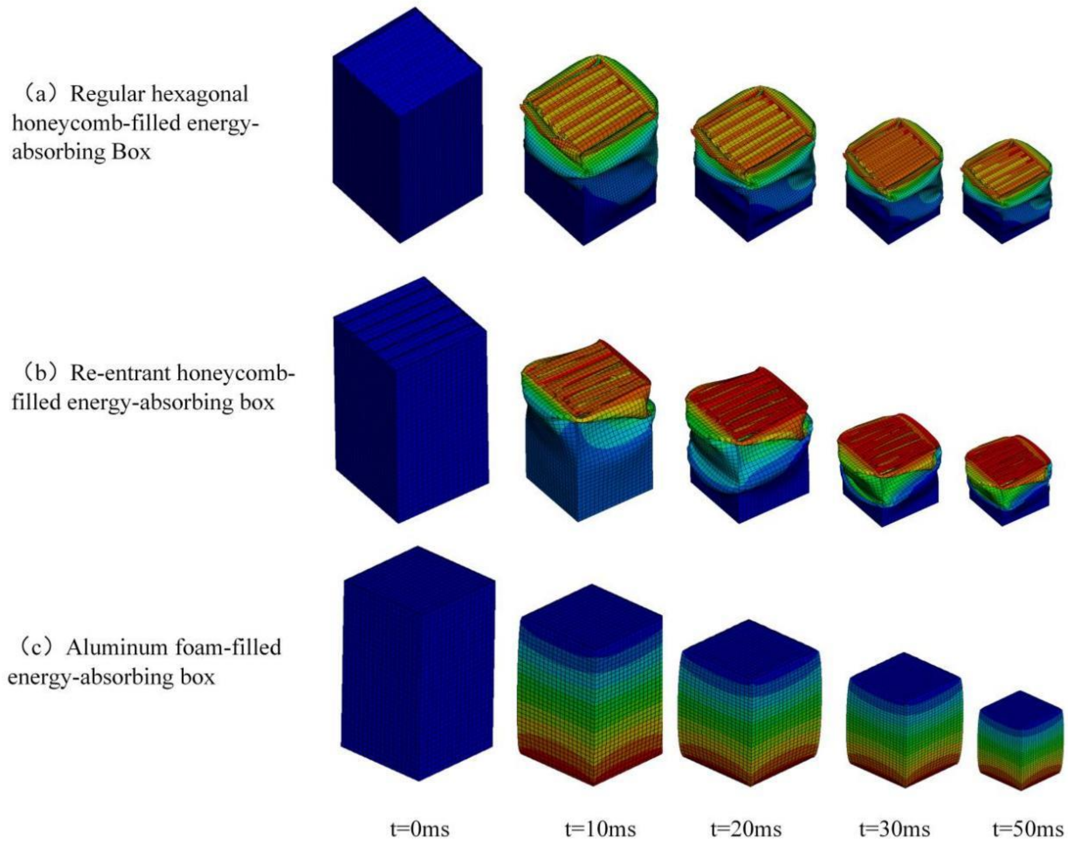

Figure 11. Deformation modes of honeycomb-filled energy-absorbing boxes during low-speed crash simulation. **(a)**regular hexagonal honeycomb-filled energy-absorbing box; **(b)** re-entrant honeycomb-filled energy-absorbing box; **(c)** Aluminum foam-filled energy-absorbing box.

To verify the crashworthiness of the honeycomb-filled energy-absorbing box, the original unfilled structure was included in the comparison. As shown in Figure 12, the load-time curves of the regular hexagonal honeycomb-filled, re-entrant honeycomb-filled, and aluminum foam-filled boxes are compared with that of the unfilled square benchmark. The corresponding energy-time curves are provided in Figure 13, and a quantitative comparison of evaluation parameters is summarized in Table 8.

Analysis of Figure 12 revealed that the peak crash load increases after filling with any of the three materials. Notably, the aluminum foam-filled structure exhibits the highest initial peak load (198 kN, Table 8) and shows considerable load fluctuations throughout the crushing process. This suggests that the aluminum foam filler may induce higher deceleration during the initial collision phase, potentially affecting occupant comfort, and demonstrates inferior load stability compared to the PEEK honeycomb-filled designs. In contrast, the increase in peak load for the PEEK honeycomb-filled boxes is minimal and remains within the permissible limit of 180 kN [37]. Furthermore, the load drops to zero earlier for all filled boxes than for the unfilled one, indicating a shorter energy absorption duration and a reduced compression stroke. A high-performance energy-absorbing box should maintain the peak load within an acceptable range while maximizing the average load to ensure energy absorption potential. The average loads of the regular hexagonal and re-entrant honeycomb-filled boxes are 68.04 kN and 64.49 kN, respectively, representing increases of 10.44 kN and 6.89 kN over the unfilled square box (57.60 kN). These results demonstrate that both PEEK honeycomb configurations effectively enhance the crashworthiness of the energy-absorbing box, offering a more stable load response than the aluminum foam filler.

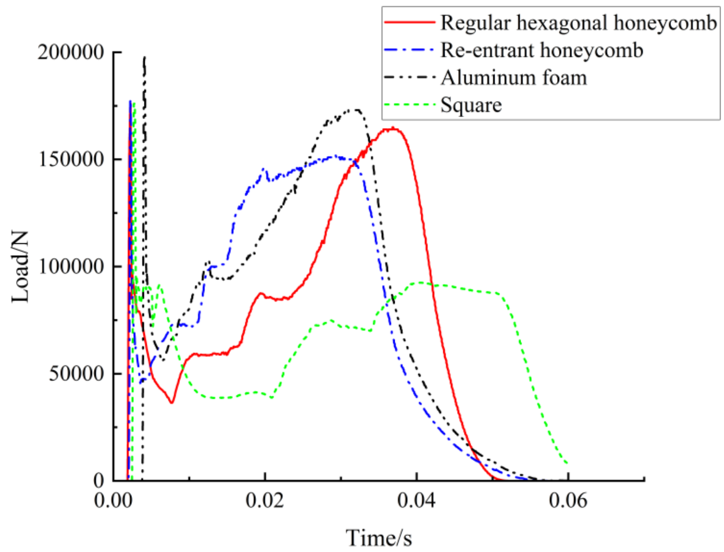

Figure 12. Load-time curves for honeycomb-filled and unfilled square energy-absorbing boxes.

As shown in Figure 13, the energy absorption curve of the energy-absorbing box during a low-speed crash can be divided into three distinct stages: initial, main energy absorption, and completion stages [38]. In the initial stage (0–10 ms), all four box configurations exhibit essentially identical energy absorption. With increasing compression displacement, the systems enter the main energy absorption stage. Here, the duration differs significantly among configurations. The PEEK honeycomb-filled boxes require less time to complete energy absorption than both the unfilled and aluminum foam-filled boxes, demonstrating superior energy absorption efficiency. Throughout this phase, the energy curves of the two PEEK honeycomb-filled boxes consistently exceed those of the unfilled square box and the aluminum foam-filled box at identical time increments, indicating greater energy absorption rates. The aluminum foam-filled structure shows a total absorbed energy closest to the unfilled box but achieves this over a longer duration. Notably, the regular hexagonal PEEK honeycomb-filled box exhibits a smooth, steadily rising energy curve, signifying progressive energy absorption through layer-by-layer buckling without violent fluctuations, a characteristic not as pronounced in the aluminum foam's curve. In the completion stage, absorbed energy plateaus for all configurations, confirming full energy dissipation. The total absorbed energy of the PEEK honeycomb-filled boxes is lower than that of the unfilled and aluminum foam-filled boxes. This reduction occurs primarily because the filling introduces additional interfacial friction and other dissipation mechanisms during compression, thereby reducing the net energy absorbed by the structural deformation itself.

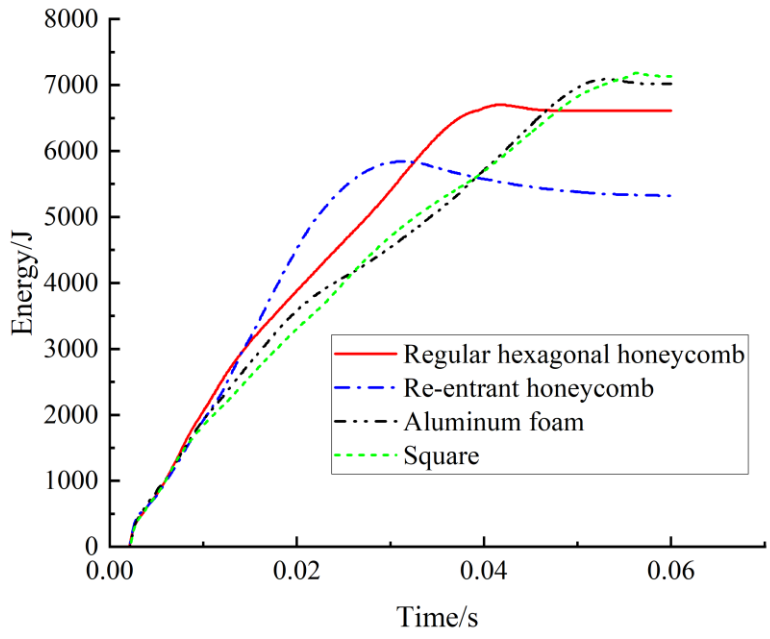

Figure 13. Energy-time curves for honeycomb-filled and unfilled square energy-absorbing boxes.

According to the simulation results in Table 8, although the specific energy absorption (SEA) of all filled structures decreased compared to the unfilled aluminum alloy box due to increased mass, each filler introduced distinct engineering trade-offs. The aluminum foam-filled structure achieved the highest total energy absorption (7060 J) among the filled designs, closely matching the unfilled box, with a compression displacement (110.34 mm) intermediate between the two PEEK honeycombs. However, it exhibited significant drawbacks: its mass was the highest (912.56 g), resulting in the lowest SEA (7.74 J/g), and it generated the highest peak load (198 kN), which is detrimental to the protection of vehicle components. In contrast, the two PEEK honeycomb-filled structures, with considerably lower mass (≈ 740–745 g), offered a more favorable performance balance. Specifically, the regular hexagonal PEEK honeycomb-filled structure provided a significantly higher mean crushing force (68.04 kN, an 18.1% increase over the unfilled box) and a compression displacement that was reduced by 26.18 mm compared to the unfilled box, indicating superior spatial energy absorption efficiency. This means it can dissipate more energy within a limited deformation distance, thereby preserving greater survival space for the occupant cabin. Although its total energy absorption (6700 J) is slightly lower than that of the aluminum foam filler, the regular hexagonal PEEK honeycomb-filled structure demonstrates a better overall balance by excelling in peak load control, lightweighting, and structural stability, making it a superior alternative to traditional aluminum foam filling under spatial constraints.

Table 8. Comparison of simulation results of different honeycomb-filled structures with unfilled energy-absorbing boxes.

Absorber box	Mass (g)	Peak load (kN)	Compression displacement (mm)	Total energy absorption (J)	Specific absorption energy (J/g)	Average load (J/mm)
Square Energy Absorbing Box	310.86	174	124.65	7180	23.09	57.60
Re-entrant honeycomb Filled Energy Absorbing Box	745.37	178	90.56	5840	7.83	64.49
Hexagonal Filled Energy Absorbing Box	740.87	176	98.47	6700	9.04	68.04
Aluminum Foam-Filled Energy Absorbing Box	912.56	198	110.34	7060	7.74	63.98

5. Prospects and challenges for engineering application

Although the simulation results demonstrate significant advantages of the PEEK regular hexagonal honeycomb-filled structure, its practical engineering application still faces several challenges, while also presenting promising directions for future advancement, as discussed below.

5.1. Manufacturing process

PEEK honeycomb structures can be fabricated via injection molding or additive manufacturing (e.g., fused deposition modeling, FDM). However, certain challenges remain in these processes, such as: FDM-based printing of PEEK requires high-temperature environments (typically above 300 °C) to ensure material melting and flow, which increases equipment complexity and energy consumption [39]. Additionally, achieving sufficient interlayer bonding strength in 3D-printed PEEK components remains a critical issue—inadequate interlayer adhesion could potentially lead to premature delamination during crash loading, undermining the structural integrity and energy absorption performance of the honeycomb filler. Future efforts should focus on optimizing printing parameters (e.g., layer height, nozzle temperature, and dwell time) or modifying PEEK with functional additives to enhance interfacial bonding.

5.2. Cost considerations

The raw material cost of PEEK is generally higher than that of common polymers (e.g., polypropylene) or aluminum foam, which may limit its large-scale industrial application in low-cost automotive scenarios. Nevertheless, the lightweight advantage of PEEK (density ~1.28 g/cm^3, approximately one-third that of aluminum alloys) and its high specific energy absorption (SEA) can translate to system-level cost benefits: lighter energy-absorbing boxes reduce overall vehicle weight, thereby improving fuel efficiency or extending battery range for new energy vehicles. With the maturation of PEEK mass production technologies and the expansion of application scales, the cost of PEEK materials is expected to decrease gradually, enhancing its economic competitiveness.

5.3. Durability and environmental adaptability

PEEK inherently exhibits excellent thermal stability, chemical corrosion resistance, and fatigue performance, which are essential for long-term service in automotive environments, as confirmed by its material properties used in this study (Table 7) and literature [40]. However, two key aspects require further validation under actual vehicle operating conditions: (1) long-term creep behavior: PEEK may undergo time-dependent deformation under sustained static loads, which could alter the geometric configuration of the honeycomb and reduce its crashworthiness over time; (2) UV aging resistance: prolonged exposure to sunlight may cause photo-oxidative degradation of PEEK, leading to reduced mechanical strength and toughness. Future studies should conduct accelerated aging tests to evaluate the durability of PEEK honeycombs and develop protective coatings or material modifications to mitigate these issues.

5.4. Intelligent design optimization driven by deep learning

Traditional design methods for PEEK honeycomb structures are often time-consuming and limited by the number of design variables. To address this limitation, future research should leverage advanced deep learning methodologies, as proposed in [41]. Machine learning algorithms—such as convolutional neural networks for crash performance prediction and generative adversarial networks for inverse topology design—can enable multi-objective optimization of PEEK honeycombs. For instance, a CNN-based surrogate model can rapidly predict the crash response of a given honeycomb topology, avoiding the need for time-consuming finite element simulations; meanwhile, GANs can automatically generate novel honeycomb structures that meet predefined safety targets. This intelligent design approach has the potential to significantly shorten the development cycle and unlock new structural configurations that outperform traditional designs.

5.5. Programmable configurations for adaptive energy management

The development of architected metamaterials with programmable mechanical properties provides new opportunities to enhance the adaptability of PEEK honeycomb-filled energy-absorbing boxes across diverse crash scenarios [42]. Inspired by auxetic metamaterials with double re-entrant configurations, future PEEK honeycombs could incorporate multi-level hierarchical structures or stimuli-responsive cells. For example, a multi-level PEEK honeycomb could be designed with macroscale re-entrant units for overall load distribution and microscale hexagonal units for localized energy dissipation; during a low-speed crash, the microscale units would deform first to reduce peak load, while at high speeds, the macroscale NPR structure would activate to enhance total energy absorption. Such programmable designs enable "on-demand" energy management, ensuring optimal crashworthiness across different impact conditions and further advancing the passive safety of automotive vehicles.

In summary, despite existing challenges in manufacturing feasibility and cost control, the PEEK regular hexagonal honeycomb-filled energy-absorbing box exhibits significant application potential. Future research should prioritize addressing the aforementioned challenges while exploring intelligent design and programmable configurations to fully exploit its performance advantages. Subsequent validation via pilot-scale production and physical bench tests will be critical to advancing its engineering application.

6. Conclusion

This study demonstrates the superior crashworthiness of a novel PEEK regular hexagonal honeycomb-filled energy-absorbing box, specifically designed to address the trade-off between lightweight and energy absorption in conventional designs. The principal findings are as follows:

(1) Replacing conventional automotive steel SPAH440 with aluminum alloy 6061-T6 for the energy-absorbing box shell effectively reduced the peak crash load and weight while maintaining energy absorption capacity.

(2) Among the cross-sections investigated (square, rectangular, circular, regular hexagonal), the square cross-section exhibited superior energy absorption characteristics coupled with the lowest peak load.

(3) Although the total energy absorption (EA) of the PEEK honeycomb-filled structure experienced a slight decrease due to mechanisms like interfacial friction, it achieved a significant increase in the mean crushing load (by 18.1%) and a substantial reduction in compression displacement (by 26.18 mm). This trade-off underscores its superior energy absorption efficiency within a constrained deformation space, better aligning with the practical design requirements for automotive energy-absorbing boxes. Furthermore, when compared to the mature benchmark of aluminum foam filler, the regular hexagonal PEEK honeycomb structure achieved comparable total energy absorption while realizing significant lightweighting (approximately 19% mass reduction) and superior peak load control. These results confirm the potential advantage of the PEEK honeycomb over traditional fillers in achieving a more optimal balance between lightweighting, crashworthiness, and spatial constraints.

The findings confirm that the PEEK regular hexagonal honeycomb-filled structure presents a superior alternative to traditional designs, particularly under spatial constraints, thereby contributing to enhanced automotive passive safety.

Authors' contribution

Conceptualization, Wenqiang Yue and Xinlin Wang; Methodology, Xinlin Wang and Wenqiang Yue; Software, Wenqiang Yue; Validation, Wenqiang Yue, Xinlin Wang and Xiaochi Wang; Formal analysis, Wenqiang Yue; Investigation, Wenqiang Yue; Resources, Tianmin Guan; Data curation, Wenqiang Yue; Writing—original draft preparation, Wenqiang Yue; Writing—review and editing, Xinlin Wang and Xiaochi Wang; Visualization, Wenqiang Yue; Supervision, Xinlin Wang; Project administration, Xinlin Wang; Funding acquisition, Xinlin Wang. All authors have read and agreed to the published version of the manuscript.

Conflicts of interests

The authors declare no conflict of interest.

References

[1] Bai Y, Yu W, Li X, Yao S, Zhang Z, *et al.* Innovative design of energy-absorbing box with hexagonal honeycomb core and its energy-absorbing characteristics (In Chinese). *J. Mech. Eng.* 2023, 50(8):26–31.

[2] Wang D, Wu Q, Shi Y, Wang Z, Liu Y. Design of automated analysis system for collision performance of labelled rectangular energy-absorbing box (In Chinese). *Heilongjiang Metall.* 2017, 37(2):60–62.

[3] Gibson LJ, Ashby MF. *Cellular solids: Structure and properties.* Cambridge: Cambridge University Press, 1997.

[4] Li X, Cao X, Yang W, Wang Y, Zhang Z. Crashworthiness of foam-filled honeycomb sandwich structures (In Chinese). *J. Wuhan Univ. Sci. Technol.* 2021,44(1):20–26.

[5] Gan NF, Wang DH, Feng YN, Wang CG, Liu LB. Numerical simulation and experimental verification of energy absorption properties of polyurethane foam-filled carbon fiber reinforced composite conical tubes (In Chinese). *China J. Mech. Eng.* 2018, 29(5):609–615.

[6] Peng XS. Process optimization of 3D printed fiber reinforced composites and study on energy absorption characteristics of automotive honeycombs (In Chinese). Master's Thesis, Dalian University of Technology, 2020.

[7] Costas M, Morin D, Langseth M, Romera L, Díaz J. Axial crushing of aluminum extrusions filled with pet foam and gfrp. An experimental investigation. *Thin-Walled Struct*. 2016, 99:45–57.

[8] Xiong Z, Cheng G. A comparative study of energy absorption characteristics of foam-filled and multi-cell square columns. *Int. J. Impact Eng.* 2007, 34(11):1739–1752.

[9] Chen W, Wierzbicki T. Relative merits of single-cell, multi-cell and foam-filled thin-walled structures in energy absorption. *Thin-Walled Struct.* 2001, 39(4):287–306.

[10] Liu Y. Study on energy absorption characteristics of aluminum foam-filled energy absorbing boxes in vehicle collisions (In Chinese). Master's Thesis, Liaoning Technical University, 2017.

[11] Hanssen AG, Hopperstad OS, Langseth M. Bending of square aluminum extrusions with aluminum foam filler. *Acta Mech.* 2000, 142:13–31.

[12] Zhao C, Zhong J, Wang H, Liu C, Li M, *et al.* Impact behaviour and protection performance of a CFRP NPR skeleton filled with aluminum foam. *Mater. Des.* 2024, 246:113295.

[13] Mohammadiha O, Beheshti H, Aboutalebi FH. Multi-objective optimisation of functionally graded honeycomb filled crash boxes under oblique impact loading. *Int. J. Crashworthiness* 2015, 20(1):44–59.

[14] Wu C, Liu Z. Protective effect of graded density aluminum foam on RC slab under blast loading—an experimental study. *Constr. Build. Mater.* 2016, 111:209–222.

[15] Xu SF. Study on low-speed impact resistance of aluminum foam sandwich structures (In Chinese). Master's Thesis, Harbin Institute of Technology, 2016.

[16] Reid SR, Reddy TY, Gray MD. Static and dynamic axial crushing of foam-filled sheet metal tubes. *Int. J. Mech. Sci.* 1986, 28(5):295–322.

[17] Yang Y. Integrated design methodology of 3D printed carbon fiber reinforced composite automotive energy-absorbing box (In Chinese). Master's Thesis, Dalian University of Technology, 2020.

[18] Quan C, Han B, Hou ZH, Zhang Q, Tian XY, *et al.* 3D printed continuous fiber reinforced composite auxetic honeycomb structures. *Compos. Part B-Eng.* 2020, 187:107858.

[19] Li MH, Wang PF, Zeng WH, Luo J, Zhang Y. Simulation analysis of low-speed collision of multi-cellular structure of energy-absorbing box of automobile (In Chinese). *J. Intern. Combust. Engines Access.* 2025, 54(4):10–12.

[20] Liu WH. Research on influencing factors of crash beam energy absorption box performance in vehicle collisions (In Chinese). Master's Thesis, Hebei University of Engineering, 2023.

[21] Wan XM, Xu XF, Xu ZM, Wang Y, Hu P. Structural optimization design of aluminum alloy automotive energy-absorbing boxes (In Chinese). *J. Automot. Eng.* 2013, 3(1):15–21.
[22] Chen YY, Zheng L. Simulation optimisation of automotive frontal collision safety based on agent model. *J. Automot. Eng.* 2018, 40(6):673–678,718.
[23] Peng, Y., Wang, S., Yao, S., & Xu, P. (2017). Crashworthiness analysis and optimization of a cutting-style energy absorbing structure for subway vehicles. *Thin-Walled Structures, 120,* 225–235.
[24] Lu H, Wang XP, Chen TN. Design and crashworthiness of a new type of energy-absorbing box with 3D negative Poisson's ratio structural filling (In Chinese). *J. Xi'an Jiaotong Univ.* 2024, 58(10):188–198.
[25] Jones DP, Leach DC, Moore DR. Mechanical properties of poly(ether-ether-ketone) for engineering applications. *Polymer* 1985, 26(9):1385–1393.
[26] Wang T. Study on mechanical properties of negative Poisson's ratio structures and application to optimal design of commercial vehicles for crashworthiness (In Chinese). Master's Thesis, Nanjing University of Science and Technology, 2017.
[27] Guo Q. Numerical simulation and experimental research on plastic forming of automobile V302 subframe (In Chinese). Master's Thesis, Nanjing University of Aeronautics and Astronautics, 2018.
[28] Zhu G. Design and analysis of bumper energy-absorbing box based on novel dot matrix structure (In Chinese). Master's Thesis, Harbin Institute of Technology, 2020.
[29] Gong J, Zhang JH, Huang SL, Liu FW. Analysis of the influence of main control parameters in PAM-CRASH collision simulation. *J. Vib. Shock.* 2002, 21(3):112–119.
[30] Zhang Y, Li Z, Pan F, Wang D, Liu J, *et al.* Crashworthiness analysis of composite structures using geometric strain-based deletion. *Compos. Struct*. 2021, 276:114552.
[31] Livermore Software Technology Corporation (LSTC). (2021). *LS-DYNA R13.0 Keyword User's Manual, Volume I*. Livermore, California, USA. Available: https://www.dynasupport.com/manuals (accessed on 18 May 2025).
[32] Livermore Software Technology Corporation (LSTC). (2018). *LS-DYNA R11.2.1 Theory Manual*. Livermore, California, USA. Available: https://www.dynasupport.com/manuals (accessed on 18 May 2025).
[33] Herbert EG, Pharr GM, Oliver WC, Lucas BN, Hay JL, *et al.* On the measurement of stress-strain curves by spherical indentation. *Thin Solid Films* 2001, 398:331–335.
[34] Zhang YW, Liu T, Tizani W. Experimental and numerical analysis of dynamic compressive response of Nomex honeycombs. *Compos. Part B-Eng.* 2018, 148:27–39.
[35] Yu I. In-plane compressive mechanical behaviour of metallic hierarchical honeycomb structures (In Chinese). Master's Thesis, Taiyuan University of Technology, 2018.
[36] Li Z. Mechanical properties of modular honeycomb structure and crashworthiness of automotive honeycomb energy-absorbing box (In Chinese). Master's Thesis, Nanjing University of Science and Technology, 2021.
[37] Zhang Y. Optimised design of automotive energy absorbing box structure under low-speed collision (In Chinese). Master's Thesis, Dalian University of Technology, 2019.
[38] Li Y. Simulation of structural energy absorbing box design and multi-objective optimization (In Chinese). Master's Thesis, Nanjing University of Aeronautics and Astronautics, 2019.
[39] Wang Y, Zhang Z, Wang X, Zhang X, Chen P, *et al.* A review on additive manufacturing of polyether

ether ketone (PEEK) composites. *Compos. Part B-Eng*. 2023, 258:110711.
[40] Kurtz SM. An overview of PEEK biomaterials. In *PEEK Biomaterials Handbook*, 2nd ed. Boston: William Andrew Publishing, 2019. pp. 3–12.
[41] He L, Li Y, Torrent D, Zhuang X, Rabczuk T, *et al.* Machine learning assisted intelligent design of meta structures: a review. *Microstructures* 2023, 3:2023037.
[42] Zhao CF, Meng ZQ, Yi JL, Chen CQ. Auxetic metamaterials with double re-entrant configuration. *Int. J. Mech. Sci*. 2025, 301:110505.